Selectivity Control in Palladium-Catalyzed Alcohol Oxidation through Selective Blocking of Active Sites

Sebastiano Campisi,[†] Davide Ferri,[‡] Alberto Villa,[†] Wu Wang,[§] Di Wang,[∥] Oliver Kröcher,[‡,⊥] and Laura Prati*,[†]

[†]Dipartimento di Chimica, Università degli Studi di Milano, Via Golgi 19, I 20133 Milano, Italy

[‡]Paul Scherrer Institut, CH 5232 Villigen, Switzerland

[§]Institute of Nanotechnology and [∥]Institute of Nanotechnology and Karlsruhe Nano Micro Facility, Karlsruhe Institute of Technology, Hermann von Helmholtz Platz 1, D 76344 Eggenstein Leopoldshafen, Germany

[⊥]Institute of Chemical Sciences and Engineering, Ecole Polytechnique Fédérale de Lausanne (EPFL), CH 1015 Lausanne, Switzerland

ABSTRACT: Stabilized metal nanoparticles (NPs) have received wide interest in a number of liquid phase catalytic transformations, but the role of the capping/protective agent is still debated. Operando attenuated total reflection infrared (ATR IR) spectros copy enabled us to obtain unprecedented molecular level insights into the selectivity issue induced by the presence of the protective agent by following the liquid phase benzyl alcohol oxidation on Pd/Al$_2$O$_3$. Supported Pd NPs protected by poly(vinyl alcohol) (PVA) showed a lower rate of benzaldehyde decarbonylation compared to unprotected Pd nanoparticles and, as a result, an improved selectivity toward the aldehyde. In addition, also the further oxidation of benzaldehyde to benzoic acid was reduced by the presence of PVA. In combination with considerations on adsorption site occupancy from CO adsorption, we ascribed this behavior to a selective blocking operated by PVA especially of Pd(111) facets, which are active in the decarbonylation process of benzaldehyde during benzyl alcohol dehydrogenation.
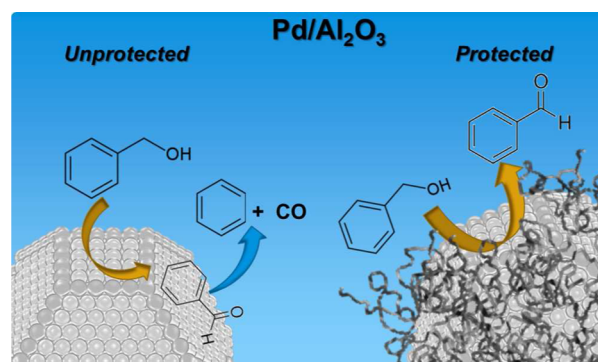
INTRODUCTION

Supported noble metal nanoparticles (e.g., Pt, Pd, and Au NPs) have been widely investigated as catalysts.[1−4] Extensive efforts have been undertaken to study the correlation between the structure of the active site and the catalytic performance. This feature assumes a primary importance in structure sensitive reactions, where the size and morphology of metal nano particles have a strong influence on the catalytic process. In these cases a single atom behaves differently depending on its position within the particle structure. Therefore, from this perspective, the rational design of morphology and size controlled nanostructures becomes increasingly important for producing very active and especially very selective catalysts.

Compared to other catalyst preparation methods, sol immobilization[5] possesses numerous advantages, including the control of the metal particle size rather irrespective of the type of support and the improvement of catalyst resistance to deactivation.[6] The key point of this synthesis route is to use protective agents (e.g., polymers or surfactants) that are necessary to form stable metallic sols and to prevent their growth or aggregation.[5,6] Because of the presence of the protective agent, at comparable metal dispersion, catalysts derived from metal sol immobilization typically exhibit lower activity than catalysts with unprotected metal nanoparticles as for instance those obtained by impregnation.[7] This behavior was mainly ascribed to the shielding effect of active sites operated by the protective agent. However, it was recently observed that the role of the protective agent is more complex. In polyvinylpyrrolidone (PVP) protected Au NPs supported on SiO$_2$ an electronic promoting effect was detected for some specific metal/PVP ratio in benzyl alcohol oxidation.[8] Furthermore, the presence of a capping agent can induce selectivity variations through direct or steric interactions with reactants.[7−15] A beneficial effect of the presence of the protective agent has been observed for supported Au, Pt, and Pd NPs in different reactions, e.g., hydrogenation of 1 epoxy 3 butene to 1 epoxybutane,[16] cynnamaldehyde hydrogena tion,[10,13,17] furfural hydrogenation,[10] and alcohol oxidation.[18,19]

We also recently observed that PVA affects the selectivity of TiO$_2$ supported Au NPs in glycerol oxidation by creating a porous like structure, where the OH groups of PVA interact

with the analogous groups of glycerol, thus directing the contact between the active site and the reactant.[7]

Despite this knowledge, the role of the protective agent is still ambiguous. The use of *in situ* techniques can be helpful in giving a more comprehensive understanding by enabling the investigation of the catalyst surface under working conditions and to recognize structure and accessibility of active sites as well as interactions with adsorbates.[20] Attenuated total reflection infrared (ATR IR) spectroscopy emerged as an ideal tool for this sort of studies, allowing to probe molecular interactions at the solid−liquid interface generated by the contact of the reactant solution with the catalyst surface.[21] Recently, the reaction pathways at the surface of Pd,[22−25] Pt,[26] and alloy[27] catalysts have been explored using ATR IR spectroscopy. Benzyl alcohol oxidation is often selected as model substrate to unravel mechanistic aspects of the liquid phase alcohol oxidation. At the current state of knowledge, the selective transformation of benzyl alcohol to benzaldehyde occurs according to an oxidative dehydrogenation path way.[1,11,28−30] Possible side products (following the mechanism reported in ref [31]), which can greatly affect the selectivity of the reaction, are represented by benzoic acid, benzene, benzyl benzoate, and toluene.[31] The selectivity toward each product appears to be related to the presence of specific active sites[24] and to the adsorption geometry and orientation of reactants and products.[33]

In this paper, by using operando ATR IR spectroscopy, we have obtained a molecular view of the role of the protective molecule in controlling the selectivity of the palladium catalyzed benzyl alcohol oxidation. In particular, we attributed the higher selectivity to benzaldehyde of Pd/Al_2O_3 catalyst obtained by sol immobilization of Pd(PVA) particles compared to an unprotected catalyst, to the selective blocking of Pd(111) faces operated by the protective molecules.

EXPERIMENTAL SECTION

Materials. Alumina (γ Al_2O_3, Condea Chemie), $NaBH_4$ (Fluka, >96%), poly(vinyl alcohol) (PVA) (MW = 13 000−23 000, 87−89% hydrolyzed, Aldrich), high purity water (Milli Q), and $Na_2PdCl_4\cdot2H_2O$ (Aldrich, 99.99% purity) were used for the preparation of the 5 wt % Pd/Al_2O_3 catalyst. Benzyl alcohol (Aldrich, >99%) and cyclohexane (Aldrich, >99%) were used as received for ATR IR experiments and catalytic tests. Pure gases (synthetic air, hydrogen, Ar; all of 99.999 vol % grade) and 0.5 vol % CO in Ar were supplied by PANGAS; O_2 (99.99% pure) for catalytic tests was from SIAD.

Catalyst Preparation. The 5 wt % Pd_{PVA}/Al_2O_3 catalyst was prepared by the sol immobilization method. Solid Na_2PdCl_4 (Pd 0.043 mol) and PVA solution (1% w/w) (Pd/PVA 1:0.5 w/w) were added to 100 mL of H_2O. After 3 min, $NaBH_4$ (Pd/$NaBH_4$ = 1/8 mol/mol) solution was added to the yellow brown solution under vigorous magnetic stirring. The brown Pd(0) sol was immediately formed. A UV−vis spectrum of the Pd sol was recorded to check the complete $PdCl_4^{2-}$ reduction. Within few minutes from their generation, the colloids (acidified at pH 2 by sulfuric acid) were immobilized by adding the support under vigorous stirring. The amount of support was calculated in order to obtain a final metal loading of 5 wt % (assuming quantitative loading of the metal on the support). The catalysts were filtered and washed several times and dried at 80 °C for 4 h. The 5 wt % Pd/Al_2O_3 catalyst was provided by Johnson Matthey.

ATR-IR Spectroscopy. A thin layer of the catalysts was deposited on an internal reflection element (IRE) and was used to investigate the liquid phase oxidation of benzyl alcohol. An aqueous slurry of the catalytic material was allowed to evaporate on the ZnSe IRE (45°, 50 × 20 × 2 mm³, Crystran) in a fume hood overnight. The deposited catalyst films were highly stable under the conditions applied.

For the ATR IR measurement a home built stainless steel flow through cell serving as a continuous flow reactor was mounted onto the ATR accessory (Specac) within the FT IR spectrometer (Vertex 70 V, Bruker Optics) equipped with an MCT detector cooled with liquid nitrogen. Spectra were recorded by averaging 100 scans at 4 cm^{-1} resolution. The cell was kept at 60 °C throughout the measurements. Cyclohexane solvent and benzyl alcohol in cyclohexane (0.02 M) were flown over the catalyst layer at a rate of 0.6 mL min^{-1} using a peristaltic pump located after the cell. Solutions were provided from two independent glass reservoirs. All transfer lines were of stainless steel.

In a general procedure, neat cyclohexane saturated with Ar was admitted to the cell until steady state conditions were achieved (ca. 30 min). In the case of 5 wt % Pd/Al_2O_3 a prereduction was performed *in situ* by admitting H_2 saturated cyclohexane for 30 min. Then, the solution of the alcohol in Ar saturated cyclohexane was admitted to the catalyst. After typically 40−50 min on stream, Ar was replaced by air for another 30−40 min. Finally, the catalyst was washed with Ar saturated cyclohexane for about 30 min to monitor desorption of reactants and products. ATR IR spectra were collected throughout the experiment. The outlet of the ATR IR *in situ* cell was connected to the inlet of the transmission infrared cell using 1/8 in. Teflon tubing. Online measurements were triggered independently from the ATR IR measurements. Typically, the online measurement was started few instants before admittance of the benzyl alcohol solution. Transmission infrared spectra were collected in the 4000−1000 cm^{-1} spectral range every 30 s (28 scans) at 4 cm^{-1} resolution with an Alpha FTIR spectrometer (Bruker) equipped with a 1 mm flow through liquid cell (CaF_2 windows).

DRIFTS. Diffuse reflectance infrared Fourier transform (DRIFT) spectra were collected with a Vertex 70 V spectrometer (Bruker Optics) equipped with a liquid nitrogen cooled MCT detector and a commercial mirror unit (Praying Mantis, Harrick). CO adsorption from the gas phase was followed at room temperature by admitting 50 mL/min of 5 vol % CO/Ar subsequent to dehydration for 1 h at 120 °C in Ar and by accumulating spectra over 30 min (first 100 scans, 14 s/spectrum; then 200 scans, ca. 180 s/spectrum; 4 cm^{-1} resolution). Adsorbed CO was then replaced by Ar in order to follow desorption under otherwise identical conditions. The powder samples (ca. 70 mg) were used without further dilution. Spectra were ratioed against a background spectrum recorded in Ar flow prior to admittance of CO.

All infrared spectra (ATR IR, DRIFT and transmission) are presented in absorbance units ($A = -\log(I/I_0)$) and were corrected for the contribution of atmospheric water where needed.

HRTEM. Morphology and microstructures of the catalysts were characterized by transmission electron microscopy (TEM) and high angle annular dark field (HAADF) scanning transmission electron microscopy (STEM). The powder samples of the catalysts were directly dispersed on copper grids covered with holey carbon film. A FEI Titan 80 300 image
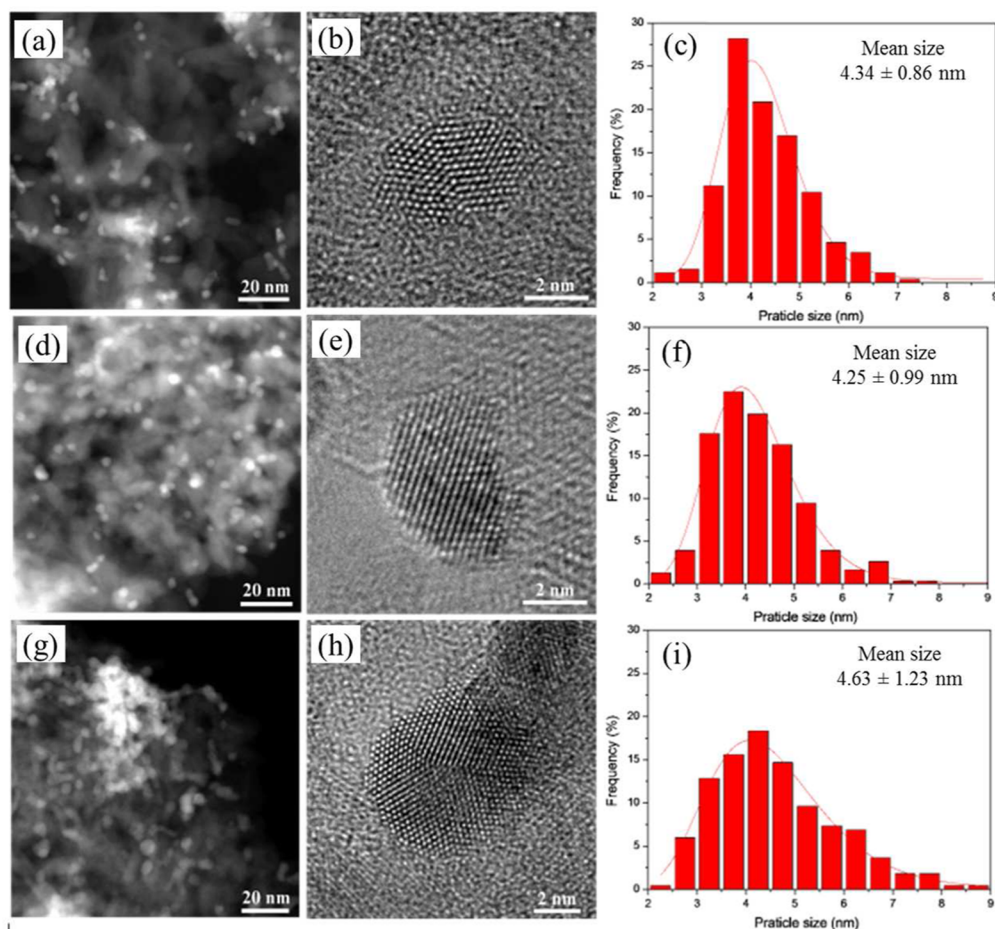
Figure 1. STEM images, HRTEM images, and particle size distributions of (a–c) 5 wt % Pd/Al$_2$O$_3$, (d–f) 5 wt % Pd$_{PVA}$/Al$_2$O$_3$, and (g–i) calcined 5 wt % Pd$_{PVA}$/Al$_2$O$_3$.

aberration corrected electron microscope operating at 300 kV was used for TEM and STEM imaging.

Catalytic Test in Batch Reactor. The reactions were carried out in a glass reactor (30 mL) provided with an electronically controlled magnetic stirrer connected to a large reservoir (5000 mL) containing oxygen at 2 bar.

The oxygen uptake was followed by a mass flow controller connected to a PC through an A/D board, plotting a flow/time diagram. For the oxidation experiments a 2.5 M solution of benzyl alcohol was used, in the presence of cyclohexane as solvent, the substrate/metal ratio was 5000 mol/mol, and the reactor was maintained at 60 °C and pressurized at p_{O_2} = 2 bar. Periodic removal of samples from the reactor was performed. Mass recoveries were always 98 ± 3% with this procedure. For the identification and analysis of the products, a GC HP 7820A gas chromatograph equipped with a capillary column (HP 5, 30 m × 0.32 mm, 0.25 μm film, made by Agilent Technologies) and TCD detector was used. Quantification of the reaction products was done by the external standard method (using 1 octanol as external standard).

RESULTS AND DISCUSSION

Pd nanoparticles (PdNPs) supported on γ Al$_2$O$_3$ (Pd$_{PVA}$/Al$_2$O$_3$) were prepared by the immobilization on the metal oxide support of preformed NPs obtained by reduction of the Pd(II) salt in the presence of poly(vinyl alcohol) (PVA) as a protective agent. For comparison, commercial unprotected PdNPs on γ Al$_2$O$_3$ (Pd/Al$_2$O$_3$) were also considered as the reference.

STEM overview images and the statistic measurement of the particle size of 5 wt % Pd/Al$_2$O$_3$ and 5 wt % Pd$_{PVA}$/Al$_2$O$_3$ are reported in Figure 1. From inspection of various images and the particle size distributions, we inferred that the two catalysts exhibited very similar metal dispersion and a mean size centered around 4 nm (Figure 1). This information justified the comparison between the two materials.

Diffuse reflectance infrared spectroscopy (DRIFTS) was first used to explore the accessibility of metal sites by monitoring the adsorption of CO as the probe molecule.

The DRIFT spectra of CO adsorbed on 5 wt % Pd/Al$_2$O$_3$ from impregnation and on 5 wt % Pd$_{PVA}$/Al$_2$O$_3$ from sol immobilization are reported in Figures 2a and 2b, respectively. Adsorbed CO on Pd/Al$_2$O$_3$ (Figure 2a) exhibits three main signals that we assigned on the basis of the literature.[34] The signal at 2098 cm^{-1} is due to CO linearly bound to Pd particle corners (CO$_L$). The signal at 1980 cm^{-1} is related to μ_2 bridge bonded CO on Pd(100) facets, while that at 1935 cm^{-1} is attributed to μ_2 bridge bonded CO on (111) planes. The DRIFTS spectrum of 5 wt % Pd$_{PVA}$/Al$_2$O$_3$ (Figure 2b) also exhibits the CO$_L$ signal at 2098 cm^{-1} and a broad feature in the region between 2050 and 1850 cm^{-1}. Three components can be identified in the latter signal. The high energy component corresponds to the signal at 1980 cm^{-1} observed on 5 wt % Pd/Al$_2$O$_3$ (Figure 1a). However, the other two components
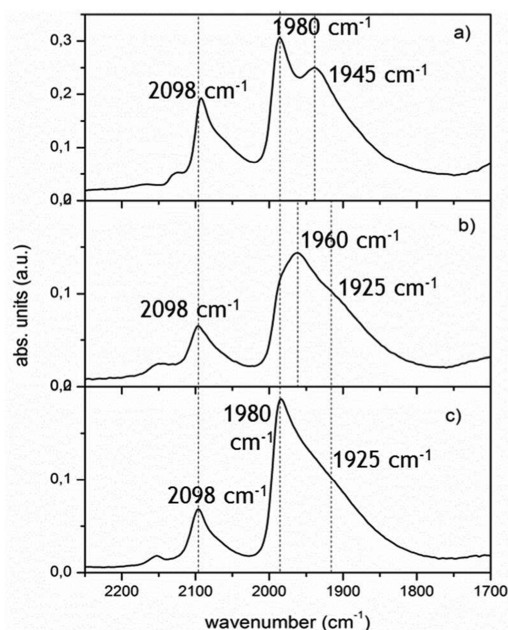
Figure 2. DRIFT spectra of adsorbed CO on (a) 5 wt % Pd/Al_2O_3, (b) 5 wt % Pd_{PVA}/Al_2O_3, and (c) calcined 5 wt % $Pd_{(PVA)}/Al_2O_3$.

centered at 1960 and 1925 cm^{-1} are clearly absent on 5 wt % Pd/Al_2O_3.

We associated these signals to a perturbation of the two components related to the CO μ_2 bridge bonded on Pd(100) and Pd(111) sites as a result of the presence of PVA. We consider that PVA acts as electron donor and influences the back donation from Pd to the π^* antibonding orbitals of CO, thus lowering the vibrational frequency of adsorbed CO.[35] This is in agreement with a recent observation that the presence of PVA induces a shift in the frequency of adsorbed CO on Au particles in 1 wt % $Au(PVA)/TiO_2$.[36] To confirm our assignment, we partially removed by gentle calcination the protective agent from Pd_{PVA}/Al_2O_3. We used a relatively low temperature (200 °C in air for 1 h) in order not to perturb the size and morphology of the Pd particles, even if under these conditions only a partial removal of PVA was expected.[37] HR TEM images (Figures 1d−f) confirmed that the calcination produced only a slight increase in mean particle size with a slight broadening of the size distribution. However, the overall morphology remained intact. When looking closely at the particle surface, the calcined Pd PVA particles are often decorated with some ill defined material, probable residual from PVA. Correspondingly, we observed that the signal at 1960 cm^{-1} disappeared in the DRIFT spectrum of the calcined sample (Figure 2c), while the one at 1980 cm^{-1} was restored, thus confirming our assignment of the 1960 cm^{-1} signal as a perturbation of the μ_2 bridge bonded CO on Pd(100). On the contrary, the signal at 1925 cm^{-1} was still present. These data indicate that PVA does not perturb CO adsorption on corners/edges (linear coordination) but is able to perturb the bridge coordination on (100) and (111) planes. Also, the interaction of PVA is stronger and more quantitative with Pd(111) than with Pd(100). Unfortunately the statistics of the different exposed facets for the catalysts is not obtained by TEM mainly due to the randomly oriented particles which not always allowed the (111) facet's identification.

The similar metal dispersion revealed by STEM (Figure 1) encouraged us to attribute the overall lower intensity of the

signals of adsorbed CO obtained on 5 wt % Pd_{PVA}/Al_2O_3 to a lower fraction of Pd atoms available for CO adsorption because of the coordination of PVA to the Pd particles.

The shielding effect produced by PVA also affected the catalytic activity for benzyl alcohol oxidation, which was measured in a glass batch reactor. The reaction profiles (conversion vs time) of Figure 3 evidenced a reduced activity of Pd_{PVA}/Al_2O_3 compared to the Pd/Al_2O_3 catalyst, in agreement with the effect of the protective agent reported earlier.[7]
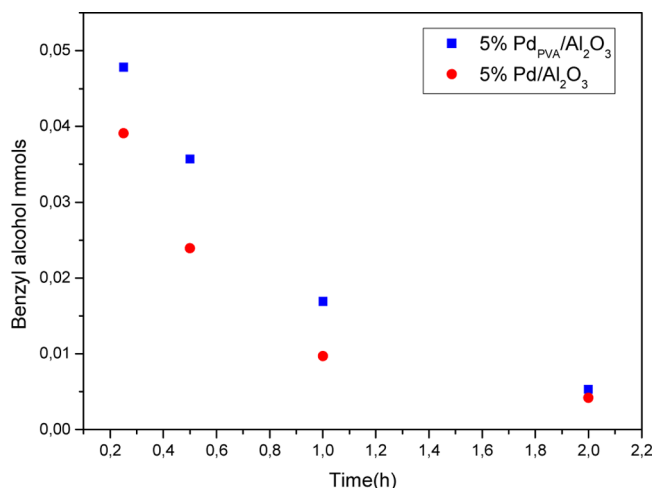
Figure 3. Reaction profiles for benzyl alcohol oxidation over 5 wt % Pd/Al_2O_3 and 5 wt % Pd_{PVA}/Al_2O_3. Reaction conditions: $C_{alcohol}$ = 2.5 M in cyclohexane; alcohol/metal = 5000 mol/mol, 60 °C, p_{O_2} = 2 bar, 1250 rpm.

More important, PVA exerted a beneficial effect on selectivity by increasing benzaldehyde production (86%, Table 1) compared to the unprotected nanoparticles (78%).

Table 1. Comparison of Activities of the Al_2O_3 Supported Pd Catalysts for Liquid Phase Benzyl Alcohol Oxidation

catalysts[a]	selectivity[b] (%)				
	toluene	benzaldehyde	benzoic acid	benzene	benzyl benzoate
5% Pd/Al_2O_3	3	78	15	3	2
5% Pd_{PVA}/Al_2O_3	6	86	4	<1	<1

[a]Reaction conditions: $C_{alcohol}$ = 2.5 M in cyclohexane, alcohol/metal = 5000 mol/mol, 60 °C, p_{O_2} = 2 bar, 1250 rpm, t = 1 h. [b]Selectivity at 99% conversion.

The results obtained by DRIFTS on the effect of PVA in CO adsorption and the effect of PVA on catalytic activity prompted us to explore benzyl alcohol transformations in the liquid phase by IR spectroscopy. The catalytic behavior of the two catalytic systems was thus monitored by ATR IR spectroscopy under both dehydrogenation (Ar) and oxidative conditions (O_2, see Figure S1) in order to separate the elementary steps of the oxidative dehydrogenation.[22] The flow through cell mimicking a continuous flow reactor configuration enables a better control of the reaction environment compared to a batch reactor cell where the products accumulate on the catalyst surface.[38,39] The catalyst layer deposited on the ZnSe crystal (IRE) was kept at 60 °C while pumping benzyl alcohol in cyclohexane solution.
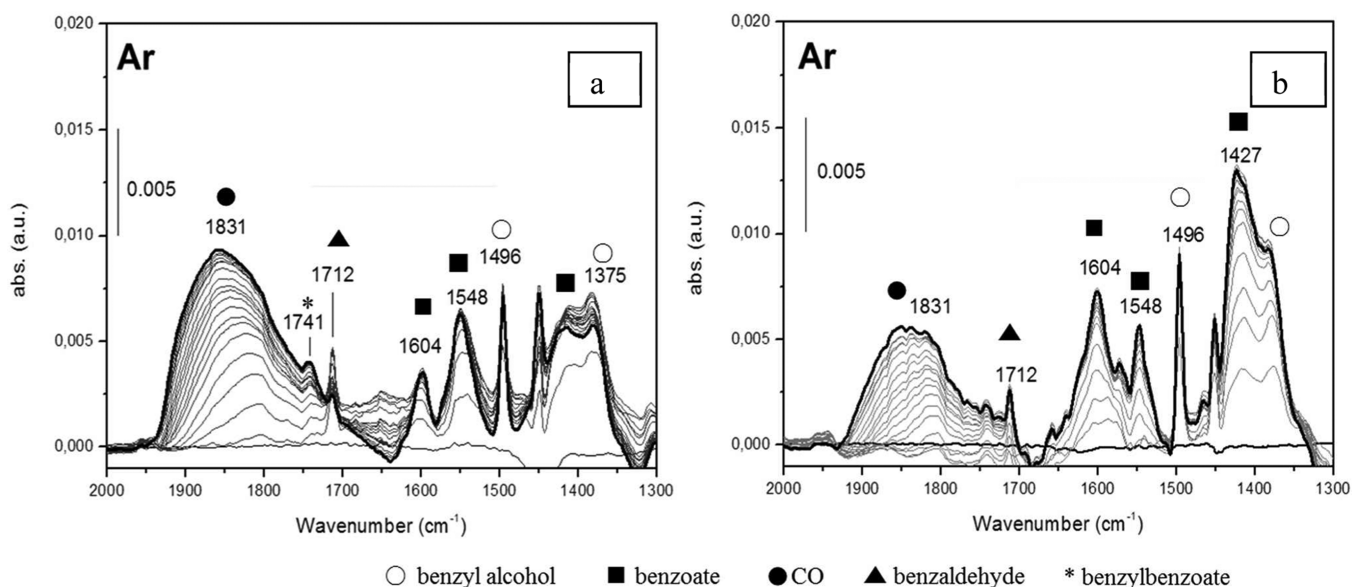
Figure 4. Operando ATR IR spectra of (a) 5 wt % Pd/Al_2O_3 and (b) 5 wt % Pd_{PVA}/Al_2O_3 in contact with a solution of benzyl alcohol under dehydrogenation conditions (Ar). Gray spectra are intermediate spectra taken at approximately similar times on stream (10 min) Conditions: $C_{alcohol}$ = 20 mM; 10 mg of catalyst; cyclohexane solvent; 60 °C; liquid flow rate = 0.6 mL/min.
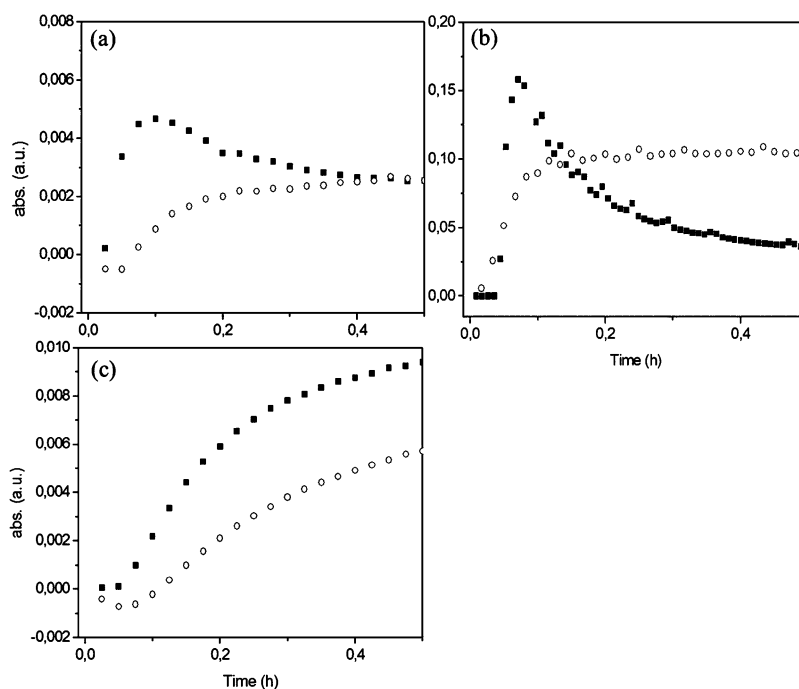
Figure 5. Time response of the signal of benzaldehyde (1712 cm^{-1}) (a) in the ATR IR and (b) in the online FTIR spectra and (c) of the ATR IR signals of adsorbed CO (1831 cm^{-1}) under dehydrogenation conditions (Ar). (■) 5 wt % Pd/Al_2O_3; (○) 5 wt % Pd_{PVA}/Al_2O_3.

The temporal evolution of the ATR IR spectra under dehydrogenation conditions (Ar) is shown in Figure 4.

The region between 1650 and 1370 cm^{-1} is dominated by signals produced by adsorbed benzoate species.[22] The intense signals at 1604 and 1427 cm^{-1} observed in Pd_{PVA}/Al_2O_3 is tentatively attributed to benzoates coordinated to the metal.[39] Benzaldehyde formation in the proximity of the surface was monitored by the sharp band at 1712 cm^{-1} corresponding to the $\nu(C=O)$ stretch mode of the carbonyl group of the aldehyde. The broad signal growing at 1806 cm^{-1} and shifting with time on stream to 1834 cm^{-1} is associated with the

evolution of CO deriving from benzaldehyde decarbonylation.[22]

Unfortunately, the second product of decarbonylation, benzene, as well as toluene from C—O bond hydrogenolysis of benzyl alcohol could not be detected since their signals are masked by the intense ones of benzyl alcohol and adsorbed benzoates. Using labeled benzyl α ^{13}C alcohol did not help to make the signals of these products more visible by exploiting the shift of the signals of adsorbed ^{13}C benzoate species.[24]

By comparing the evolution of the CO signal in the dehydrogenation segment (Figure 4a,b), it appears that benzaldehyde decarbonylation takes place at a lesser extent

on 5 wt % Pd_{PVA}/Al_2O_3 than on 5 wt % Pd/Al_2O_3. The difference is better appreciated by analyzing the temporal response of the $\nu(C{=}O)$ signal of benzaldehyde in the ATR IR spectra and in the transmission IR spectra obtained online at the exit of the cell (Figure 5 and Figure S2). The amount of benzaldehyde that is formed in the catalyst layer monitored by the infrared radiation in the ATR IR mode is different in the two catalysts. In the case of 5 wt % Pd_{PVA}/Al_2O_3, benzaldehyde production reaches a steady state value approximately after 15 min. On the contrary, benzaldehyde evolution on 5 wt % Pd/Al_2O_3 passes through a maximum before returning to the level observed for 5 wt % Pd_{PVA}/Al_2O_3. CO formation and coordination to Pd occur parallel to benzaldehyde production. CO adsorption increases during the dehydrogenation phase. The rate of growth of the signal of adsorbed CO tightly follows the evolution profile of benzaldehyde, clearly indicating that decarbonylation occurs at the beginning of the reaction with Pd/Al_2O_3.

The high amount of benzaldehyde obtained at the beginning of the reaction under dehydrogenation conditions for 5 wt % Pd/Al_2O_3 is confirmed by the temporal profile of the online infrared spectra of Figure 5b. The discrepancy detected between the amount of benzaldehyde detected at the catalyst surface (Figure 5a) and in solution (Figure 5b) is solved remembering that ATR IR spectroscopy monitors a thin layer of the catalyst (ca. 1−4 μm as a function of energy) that is identical in the two experiments. On the contrary, the online FTIR spectrometer at the exit of the cell measures the global activity of the catalyst layer deposited on the ZnSe crystal, i.e., including the portion not probed by the IR radiation. Therefore, 5 wt % Pd_{PVA}/Al_2O_3 demonstrated higher benzaldehyde production than 5 wt % Pd/Al_2O_3 under dehydrogenation conditions, in agreement with the catalytic data (Table 1).

It has been previously demonstrated using ATR IR spectroscopy that the decarbonylation occurs preferentially on Pd(111) faces.[24] Recalling the CO adsorption measurements where a preferential adsorption of PVA on these planes was evidenced, we could now correlate the two findings and address the higher production of benzaldehyde to the selective blocking, operated by PVA, of the sites responsible for benzaldehyde decomposition.

Recently, TPD HREELS experiments revealed the crucial role of the adsorption geometry of the aromatic moiety on the Pd(111) faces in the decarbonylation process.[40] The flat lying adsorption geometry adopted by benzyl alcohol molecules at low surface coverage of Pd(111) was shown to favor benzaldehyde decarbonylation,[33,40] in agreement with the interpretation of the ATR IR liquid phase benzyl alcohol oxidation experiments.[24]

The experimental results from DRIFTS and ATR IR spectroscopy pointed out that PVA molecules induce a selectivity control. We interpret this effect as an influence on molecular orientation of the adsorbates. In the proximity of PVA molecules anchored to Pd(111) faces, benzyl alcohol can adsorb with the ring away from the surface in a similar fashion to terrace edges and the Pd(100) faces where benzaldehyde is more likely formed and desorbed without decomposing.[24]

CONCLUSIONS

We have demonstrated that the presence of the protective agent PVA in catalysts prepared by metal sol immobilization is not innocent neither from activity nor selectivity standpoints.

Compared to conventional Pd/Al_2O_3, supported Pd NPs protected by PVA exhibit lower conversion levels but enhanced selectivity to benzaldehyde in the liquid phase benzyl alcohol oxidation. By monitoring the evolution of the catalyst surface by operando ATR IR spectroscopy, it was revealed that the selectivity enhancement induced by the protective agent is the result of the limited decarbonylation of the benzaldehyde product. This behavior is associated with the preferential blocking of Pd(111) facets, which have been recognized to facilitate the decarbonylation process. The possibility to influence the selectivity in alcohol oxidation by the selective blocking of specific active site represents a potential tool and an additional advantage justifying the use of supported metal nanoparticles from colloidal synthesis as catalyst.

ASSOCIATED CONTENT

● Supporting Information

The Supporting Information is available free of charge on the ACS Publications website at DOI: 10.1021/acs.jpcc.6b01549.

Experimental details and kinetic profiles (PDF)

AUTHOR INFORMATION

Corresponding Author

*E mail laura.prati@unimi.it; Tel +39 02 50314357 (L.P.).

Notes

The authors declare no competing financial interest.

REFERENCES

(1) Besson, M.; Gallezot, P. Selective Oxidation Of Alcohols And Aldehydes On Metal Catalysts. *Catal. Today* **2000**, *57*, 127−141.

(2) Mallat, T.; Baiker, A. Oxidation Of Alcohols With Molecular Oxygen On Solid Catalysts. *Chem. Rev.* **2004**, *104*, 3037−3058.

(3) Dimitratos, N.; Lopez Sanchez, J. A.; Hutchings, G. J. Selective Liquid Phase Oxidation With Supported Metal Nanoparticles. *Chem. Sci.* **2012**, *3*, 20−44.

(4) Davis, S. E.; Ide, M. S.; Davis, R. J. Selective Oxidation Of Alcohols And Aldehydes Over Supported Metal Nanoparticles. *Green Chem.* **2013**, *15*, 17−45.

(5) Prati, L.; Martra, G. New Gold Catalysts For Liquid Phase Oxidation. *Gold Bull.* **1999**, *32*, 96−101.

(6) Coluccia, S.; Martra, G.; Porta, F.; Prati, L.; Rossi, M. Metal Sols As A Useful Tool For Heterogeneous Gold Catalyst Preparation: Reinvestigation Of A Liquid Phase Oxidation. *Catal. Today* **2000**, *61*, 165−172.

(7) Villa, A.; Wang, D.; Veith, G. M.; Vindigni, F.; Prati, L. Sol Immobilization Technique: A Delicate Balance Between Activity, Selectivity And Stability Of Gold Catalysts. *Catal. Sci. Technol.* **2013**, *3*, 3036−3041.

(8) Chen, K.; Wu, H.; Hua, Q.; Chang, S.; Huang, W. Enhancing Catalytic Selectivity Of Supported Metal Nanoparticles With Capping Ligands. *Phys. Chem. Chem. Phys.* **2013**, *15*, 2273−2277.

(9) Niu, Z.; Li, Y. Removal And Utilization Of Capping Agents In Nanocatalysis. *Chem. Mater.* **2014**, *26*, 72−83.

(10) Schoenbaum, C. A.; Schwartz, D. K.; Medlin, J. W. Controlling The Surface Environment Of Heterogeneous Catalysts Using Self Assembled Monolayers. *Acc. Chem. Res.* **2014**, *47*, 1438−1445.

(11) Mallat, T.; Baiker, A. Selectivity Enhancement In Heterogeneous Catalysis Induced By Reaction Modifiers. *Appl. Catal., A* **2000**, *200*, 3−22.

(12) Pieters, G.; Prins, L. J. Catalytic Self Assembled Monolayers On Gold Nanoparticles. *New J. Chem.* **2012**, *36*, 1931−1939.

(13) Zhong, R.; Sun, K.; Hong, Y.; Xu, B. Impacts Of Organic Stabilizers On Catalysis Of Au Nanoparticles From Colloidal Preparation. *ACS Catal.* **2014**, *4*, 3982−3993.

(14) Huang, W.; Hua, Q.; Cao, T. Influence And Removal Of Capping Ligands On Catalytic Colloidal Nanoparticles. *Catal. Lett.* **2014**, *144*, 1355−1369.

(15) Gavia, D. J.; Shon, Y. S. Catalytic Properties Of Unsupported Palladium Nanoparticle Surfaces Capped With Small Organic Ligands. *ChemCatChem* **2015**, *7*, 892−900.

(16) Marshall, S. T.; O'Brien, M.; Oetter, B.; Corpuz, A.; Richards, R. M.; Schwartz, D. K.; Medlin, J. W. Controlled Selectivity For Palladium Catalysts Using Self Assembled Monolayers. *Nat. Mater.* **2010**, *9*, 853−858.

(17) Kahsar, K. R.; Schwartz, D. K.; Medlin, J. W. Control Of Metal Catalyst Selectivity Through Specific Noncovalent Molecular Interactions. *J. Am. Chem. Soc.* **2014**, *136*, 520−526.

(18) Feng, B.; Hou, Z.; Yang, H.; Wang, X.; Hu, Y.; Li, H.; Qiao, Y.; Zhao, X.; Huang, Q. Functionalized Poly (Ethylene Glycol) Stabilized Water Soluble Palladium Nanoparticles: Property/Activity Relationship For The Aerobic Alcohol Oxidation In Water. *Langmuir* **2010**, *26*, 2505−2513.

(19) Quintanilla, A.; Butselaar Orthlieb, V. C. L.; Kwakernaak, C.; Sloof, W. G.; Kreutzer, M. T.; Kapteijn, F. Weakly Bound Capping Agents On Gold Nanoparticles In Catalysis: Surface Poison? *J. Catal.* **2010**, *271*, 104−114.

(20) Weckhuysen, B. M. Determining The Active Site In A Catalytic Process: Operando Spectroscopy Is More Than A Buzzword. *Phys. Chem. Chem. Phys.* **2003**, *5*, 4351−4360.

(21) Andanson, J. M.; Baiker, A. Exploring Catalytic Solid/Liquid Interfaces By In Situ Attenuated Total Reflection Infrared Spectroscopy. *Chem. Soc. Rev.* **2010**, *39*, 4571−4584.

(22) Keresszegi, C.; Ferri, D.; Mallat, T.; Baiker, A. Unraveling The Surface Reactions During Liquid Phase Oxidation Of Benzyl Alcohol On Pd/Al$_2$O$_3$: An In Situ ATR IR Study. *J. Phys. Chem. B* **2005**, *109*, 958−967.

(23) Bürgi, T. Combined In Situ Attenuated Total Reflection Infrared And UV−Vis Spectroscopic Study Of Alcohol Oxidation over Pd/Al$_2$O$_3$. *J. Catal.* **2005**, *229*, 55−63.

(24) Ferri, D.; Mondelli, C.; Krumeich, F.; Baiker, A. Discrimination Of Active Palladium Sites In Catalytic Liquid Phase Oxidation Of Benzyl Alcohol. *J. Phys. Chem. B* **2006**, *110*, 22982−22986.

(25) Mondelli, C.; Ferri, D.; Grunwaldt, J.; Krumeich, F.; Mangold, S.; Psaro, R.; Baiker, A. Combined Liquid Phase ATR IR And XAS Study Of The Bi Promotion In The Aerobic Oxidation Of Benzyl Alcohol Over Pd/Al$_2$O$_3$. *J. Catal.* **2007**, *252*, 77−87.

(26) Ide, M. S.; Falcone, D. D.; Davis, R. J. On The Deactivation Of Supported Platinum Catalysts For Selective Oxidation Of Alcohols. *J. Catal.* **2014**, *311*, 295−305.

(27) Nowicka, E.; Hofmann, J. P.; Parker, S. F.; Sankar, M.; Lari, G. M.; Kondrat, S. A.; Knight, D. W.; Bethell, D.; Weckhuysen, B. M.; Hutchings, G. J. In Situ Spectroscopic Investigation Of Oxidative Dehydrogenation And Disproportionation Of Benzyl Alcohol. *Phys. Chem. Chem. Phys.* **2013**, *15*, 12147−12155.

(28) Vinke, P.; van Dam, H. E.; van Bekkum, H. Platinum Catalyzed Oxidation Of 5 Hydroxymethylfurfural. *Stud. Surf. Sci. Catal.* **1990**, *55*, 147−158.

(29) Kluytmans, J. H. J.; Markusse, A. P.; Kuster, B. F. M.; Marin, G. B.; Schouten, J. C. Engineering Aspects Of The Aqueous Noble Metal Catalysed Alcohol Oxidation. *Catal. Today* **2000**, *57*, 143−155.

(30) Xu, X. P.; Friend, C. M. Selective β elimination In The Reaction Of 2 Propanol To Acetone On Rh (111) p (2× 1) O. *Surf. Sci.* **1992**, *260*, 14−22.

(31) Savara, A.; Chan Thaw, C. E.; Rossetti, I.; Villa, A.; Prati, L. Benzyl Alcohol Oxidation On Carbon Supported Pd Nanoparticles: Elucidating The Reaction Mechanism. *ChemCatChem* **2014**, *6*, 3464−3473.

(32) Sankar, M.; Nowicka, E.; Miedziak, P. J.; Brett, G. L.; Jenkins, R. L.; Dimitratos, N.; Taylor, S. H.; Knight, D. W.; Bethell, D.; Hutchings, G. J. Oxidation Of Alcohols Using Supported Gold And Gold−Palladium Nanoparticles. *Faraday Discuss.* **2010**, *145*, 341−356.

(33) Pang, S. H.; Román, A. M.; Medlin, J. W. Adsorption Orientation Induced Selectivity Control Of Reactions Of Benzyl Alcohol On Pd (111). *J. Phys. Chem. C* **2012**, *116*, 13654−13660.

(34) Sheppard, N.; Nguyen, T. T. *Advances in Infrared Raman Spectroscopy*; Heyden: London, UK, Vol. 5, p 198.

(35) Ray, N. A.; Van Duyne, R. P.; Stair, P. C. Synthesis Strategy For Protected Metal Nanoparticles. *J. Phys. Chem. C* **2012**, *116*, 7748−7756.

(36) Lari, G. M.; Nowicka, E.; Morgan, D. J.; Kondrat, S. A.; Hutchings, G. J. The Use Of Carbon Monoxide As A Probe Molecule In Spectroscopic Studies For Determination Of Exposed Gold Sites On TiO$_2$. *Phys. Chem. Chem. Phys.* **2015**, *17*, 23236−23244.

(37) Lopez Sanchez, J. A.; Dimitratos, N.; Hammond, C.; Brett, G. L.; Kesavan, L.; White, S.; Miedziak, P.; Tiruvalam, R.; Jenkins, R. L.; Carley, A. F.; et al. Facile Removal Of Stabilizer Ligands From Supported Gold Nanoparticles. *Nat. Chem.* **2011**, *3*, 551−556.

(38) Ferri, D.; Baiker, A. Advances in Infrared Spectroscopy of Catalytic Solid−Liquid Interfaces: The Case of Selective Alcohol Oxidation. *Top. Catal.* **2009**, *52*, 1323−1333.

(39) Villa, A.; Ferri, D.; Campisi, S.; Chan Thaw, C. E.; Lu, Y.; Kröcher, O.; Prati, L. Operando Attenuated Total Reflectance FTIR Spectroscopy: Studies on the Different Selectivity Observed in Benzyl Alcohol Oxidation. *ChemCatChem* **2015**, *7*, 2534−2541.

(40) Williams, R. M.; Medlin, J. W. Benzyl Alcohol Oxidation on Pd (111): Aromatic Binding Effects on Alcohol Reactivity. *Langmuir* **2014**, *30*, 4642−4653.